Shape of Phospholipid/Surfactant Mixed Micelles: Cylinders or Disks? Theoretical Analysis

M. M. Kozlov,*,† D. Lichtenberg,† and D. Andelman‡

Department of Physiology and Pharmacology, Sackler School of Medicine, Tel Aviv University, Ramat-Aviv 69978, Israel, and School of Physics and Astronomy, Raymond and Beverly Sackler Faculty of Exact Sciences, Tel Aviv University, Ramat-Aviv 69978, Israel

Received: January 23, 1997; In Final Form: April 14, 1997[⊗]

We develop a theoretical model for the solubilization of phospholipid bilayers by micelle-forming surfactants. Cylindrical micelles, disklike micelles, and spherical micelles are considered as alternative resultant structures. The main question addressed is, what kind of micelles can be expected under various thermodynamical conditions? Our analysis is based on a theoretical model that accounts for Helfrich energy of curvature of amphiphile monolayers and for the entropy of mixing of lipids and surfactants in mixed aggregates. We conclude that for usual values of the elastic parameters of amphiphile monolayers cylindrical micelles are the most probable aggregates resulting from micellization of phospholipid by surfactants. This conclusion is consistent with available experimental data. Conditions of formation of disklike and spherical micelles are also determined.

Introduction

Amphiphiles tend to self-assemble in aqueous solutions, mostly due to the hydrophobic effect.[1] In the resultant aggregates, the amphiphilic molecules are packed as monolayers, where their hydrophobic moieties are shielded from contact with the external aqueous medium by the polar head groups. Depending on their molecular structure and interactions, the amphiphiles form aggregates of different shapes.[2−4] Most of the biological amphiphiles (phospholipids) self-assemble in nearly flat bilayer membranes, forming closed vesicles (liposomes). By contrast, most of the commonly used surfactants form micelles whose radii of curvature are close to the length of hydrocarbon chains.[5]

While each of the pure compounds form in dilute solution aggregates of a particular type, mixtures of lipids and surfactants self-assemble in either mixed liposomes or mixed micelles, depending on the composition.[5−7] Transition from mixed bilayers to mixed micelles upon addition of surfactant to phospholipid vesicles is commonly denoted as solubilization of the liposomes. The resultant micelles were previously described as having either disklike (oblate ellipsoidal[8]) or cylindrical shapes,[5] in apparent agreement with dynamic light scattering data.

More recently, however, cryotransmition electron microscopy,[9,10] size-exclusion high-performance liquid chromatography,[11] small angle neutron scattering,[12] and re-evaluation of dynamic light scattering data[13] indicated that in most cases solubilization of liposomes results in formation of threadlike rather than disklike micelles.

The model of disklike micelles was supported by the idea that the surfactant molecules form the rims of the micelles where the amphiphile monolayers are strongly curved, while the lipid molecules remain in flat parts of the disks. However, this qualitative consideration did not account for the entropy of mixing of the two components in the micelle, which tends to distribute uniformly the molecules of the two components over the whole surface of each micelle. The result of competition of these two tendencies is not obvious and requires a detailed theoretical analysis.

Based on the more recent experimental results, theoretical approaches that were developed to describe the energetics and size distributions of mixed amphiphilic aggregates[14,15] and to interpret the phase diagrams of lipid−surfactant mixtures[6,7] assumed that cylindrical and spherical micelles are the only possible aggregates resulting from solubilization. The question remains open whether disklike micelles are indeed less favorable energetically than the cylindrical and spherical ones and if there are conditions where solubilization can still result in formation of disklike micelles.

The present work analyzes and compares the conditions of surfactant-induced phase transition of lipid bilayers into discoidal, cylindrical, and spherical micelles. Our model, unlike alternative theoretical approaches,[16] does not consider the detailed distribution of microscopic interactions in amphiphile monolayers. Instead, we describe a monolayer of amphiphiles by the more macroscopic Helfrich elastic model and account for the lipid/surfactant entropy of mixing. We show that the shape of the micelles formed upon solubilization of liposomes is determined by a unique parameter that depends on the temperature and on the elastic characteristics of the monolayer as expressed by its bending rigidity, the spontaneous curvatures of the two compounds, and the Gaussian curvature modulus.

On the basis of our calculations, we conclude that at all reasonable values of this parameter the predicted shapes of the mixed micelles are those of long cylinders, in agreement with the recent experimental data.[9,10] Disklike micelles can only be expected for compounds whose Gaussian curvature modulus is of unusually high negative value. Another possibility of obtaining disklike micelles is to suppress the effects of the entropy of mixing by decreasing the temperature.

The Model

We consider a ternary system of water, lipid, and surfactant. The concentrations of lipid and surfactant in water, denoted by N_L and N_D, respectively, are assumed to be much higher than the critical micelle concentrations (cmc).

We consider the following states of the aqueous solution of the amphiphiles in terms of the most common shapes of the

† Sackler School of Medicine.
‡ Raymond and Beverly Sackler Faculty of Exact Sciences.
⊗ Abstract published in *Advance ACS Abstracts,* June 1, 1997.

S1089-5647(97)00295-2 CCC: $14.00

aggregates: flat bilayers (liposomes, whose radius is taken as very large in comparison to the bilayers thickness), cylindrical micelles, disklike micelles, spherical micelles, and mixtures of coexisting aggregates of these types. Since the aim of our work is to analyze qualitatively the main pathways of solubilization of bilayers, we do not consider the more complicated architecture of intermediate aggregates[17] such as ellipsoidal micelles and hyperbolic and mesh structures.[17−20] Moreover, we will assume that both lipid and surfactant are nonionic so that we will not consider any possible effects of electric charges of polar heads.[21]

To characterize the composition of the system, we use the area fraction occupied by surfactant:

$$\phi = \frac{a_D N_D}{a_D N_D + a_L N_L} \tag{1}$$

where a_D and a_L are the molecular areas of the surfactant and lipid, respectively, at the monolayer plane. It is assumed that those specific areas do not differ for aggregates of various types.

In our model, the pure lipid system ($\phi = 0$) preferentially forms liposomes, while addition of the surfactant results in transition of liposomes into micelles of one of the shapes mentioned above. To analyze the resulting structures, we determine for each of the possible aggregates mentioned above the free energy as a function of composition. Comparing those free energies, we find for each composition the state of the lowest free energy, i.e. the equilibrium structure.

The obvious difference between the structures of aggregates is the curvature of their monolayers. Therefore, as a first contribution to the free energy (per unit area) of the monolayer, u, we consider the Helfrich energy of bending u_b.[22] The other major contribution is that of the entropy of mixing of the two components in the monolayer, s.[6] Hence,

$$u = u_b - Ts$$

We neglect the translational entropy of aggregates and the entropy of polydispersity of the micellar sizes[14] since the related contribution to the free energy can be shown to correct only slightly the criteria of solubilization of the bilayers.

The energy of bending (per unit area) of the monolayer is

$$u_b = \frac{1}{2}\kappa(c_m + c_p - c_0)^2 + \bar{\kappa} c_m c_p \tag{2}$$

where c_m and c_p are the principal curvatures of the bent surface.[22] The material properties of the monolayer that determine the bending energy (2) are the bending rigidity κ, the Gaussian curvature modulus $\bar{\kappa}$, and the spontaneous curvature c_0.

The model (2) has been originally formulated for membrane shapes that deviate only slightly from a flat surface.[22] Extension of this model to the cases of strongly curved micelles can be justified by recent analysis of the elastic properties of monolayers of inverted hexagonal phases, whose curvature is comparable (but opposite in sign) to the curvature of cylindrical micelles.[23,24]

For the sake of simplicity we will assume that the moduli κ and $\bar{\kappa}$ do not depend on composition. While several theoretical models predict different characters of such dependencies,[25,26] a more recent numerical calculation[27] revealed a weak dependence of κ on the composition of a mixed membrane. Moreover, an experimental determination of the bending rigidity of mixed monolayers of H_{II} phases did not show any pronounced changes of κ with composition.[24] However, let us emphasize that this assumption can be a strong simplification, especially in the cases of mixtures of amphiphiles with different chain length. Therefore, the results of the present model should be regarded as qualitative ones indicating the main trends of phase behavior of amphiphilic mixtures rather than giving exact criteria of the phase transitions.

By contrast, the spontaneous curvature c_0 is assumed to depend strongly on the monolayer composition. Although this dependence may be rather complicated,[15,28] we will assume that c_0 is the area-weighted average of the spontaneous curvatures of pure lipid c_L and pure surfactant c_D,

$$c_0 = (1 - \phi)c_L + \phi c_D \tag{3}$$

This assumption is supported by numerical calculations[27] that showed that the spontaneous curvatuve of a monolayer consisting of surfactants with different chain lengths is a linear function of ϕ over a wide range of compositions. Furthermore, for mixed monolayers of H_{II} phases it has been shown experimentally[24] that c_0 depends linearly on ϕ.

To account for the entropy of mixing (per unit area) of the two components, we will use an approximate expression for ideal mixing:[6]

$$\frac{s}{k_B} = -\frac{1}{a_L}[\phi \log \phi + (1 - \phi) \log(1 - \phi)] \tag{4}$$

The following analysis depends mainly on the behavior of the entropy s near its minimal value at $\phi = 1/2$. Within this range (4) can be substituted by a simpler equation:

$$\frac{1}{k_B}s = -\frac{1}{a_L}[2\phi(\phi - 1) - 0.2] \tag{5}$$

Equation 5 in fact approximates (4) with good accuracy for any value of ϕ within the range $0.2 < \phi < 0.8$, which covers the whole range of "solubilizing ratios" in any lipid/surfactant mixture studied thus far.

We will assume below that the characteristic radius of the curved parts of amphiphile monolayers is equal to ρ for all kinds of aggregates. It is convenient to express all the variables in dimensionless form. The dimensionless free energy per unit area f, the dimensionless curvature ζ, and the dimensionless temperature η are defined as

$$f = \frac{2\rho^2}{\kappa}u, \quad \zeta = \rho c, \quad \text{and} \quad \eta = \frac{4k_B T\rho^2}{\kappa a_L}$$

The dimensionless energy per unit area of the monolayer is

$$f = (\zeta_m + \zeta_p - \zeta_0)^2 + 2\frac{\bar{\kappa}}{\kappa}\zeta_m\zeta_p + \eta\phi(\phi - 1) + \text{const} \tag{6}$$

where ζ_0 depends on ϕ according to (3).

Equations 1−6 are the basis for the determination of the free energies of different micellar states and liposomes (flat bilayers) as functions of their compositions.

Free Energies

Disklike Micelles. The shape of a disklike micelle is assumed to consist of a flat central part with radius R and a rim formed by a strongly curved monolayer, whose meridional principal curvature is $1/\rho$ (Figure 1). The areas of the rim and the flat part are denoted as A_e and A_f, respectively. The geometrical characteristics of the monolayer forming the rim are considered in detail in Appendix A.

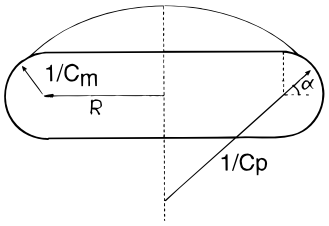

Figure 1. Schematic representation a disklike micelle. $c_m = 1/\rho$ and c_p are the meridional and parallel curvatures of the surface of the rim, respectively, and R is the radius of the flat central part of the micelle. Meridional angle α determines position along the profile of the rim.

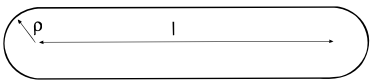

Figure 2. Schematic representation of a cylindrical micelle. l is the length of cylindrical body; ρ is the radius of curvature of the semispherical caps.

To calculate the free energy of a disklike micelle f_D as a function of its composition ϕ_D, we take into account the partitioning of the surfactant between the flat part and the rim (Appendix B) while determining the area-weighted average of the energy (6). Denoting the dimensionless total curvature in the rim as $J = (c_m + c_p)\rho$, we obtain for the free energy (per unit area)

$$f_D = [(\Delta\zeta)^2 + \eta]\phi_D^2 + \left(2\zeta_L\Delta\zeta - \eta - 2\frac{A_e}{A_t}\Delta\zeta\langle J\rangle\right)\phi_D + \frac{A_e}{A_t}\left[\frac{\eta}{\eta + (\Delta\zeta)^2}\langle J^2\rangle + \frac{(\Delta\zeta)^2}{\eta + (\Delta\zeta)^2}\langle J\rangle^2\right] - \frac{A_eA_f}{A_t^2}\frac{(\Delta\zeta)^2}{\eta + (\Delta\zeta)^2}\langle J\rangle^2 - 2\frac{A_e}{A_t}\zeta_L\langle J\rangle + \zeta_L^2 + 8\pi\frac{\bar\kappa\rho^2}{\kappa A_t} \quad (7)$$

where $\langle J\rangle$ and $\langle J^2\rangle$ are the values of the total curvature and its square, averaged over the curved area forming the rim, and $\Delta\zeta = \zeta_D - \zeta_L$ is the difference between the spontaneous curvatures of surfactant and lipid expressed in dimensionless form.

Cylindrical Micelles. We assume that all the cylindrical micelles have the same shape consisting of a cylindrical part of a length l with two semispherical caps at the ends (Figure 2). The radius of the cross section of the cylinder and of the hemispheres is assumed to be equal to ρ. The areas of the cylindrical part and the caps will be denoted as A_l and A_h, respectively, and the total area is $A_t = A_l + A_h$.

To derive the energy of the phase of cylindrical micelles (Appendix C) we first determine the partitioning of the surfactant between the less curved cylindrical body and more curved semipherical caps. Subsequently, we average the energy (6) over the area of one cylindrical micelle, including its body and two caps. As a result, we obtain the free energy per unit area as a function of the micellar composition ϕ_c:

$$f_c = [(\Delta\zeta)^2 + \eta]\phi_c^2 + (2\zeta_L\Delta\zeta - \eta - 2\Delta\zeta)\phi_c - 2\Delta\zeta\phi_c\frac{A_h}{A_t} + (\zeta_L - 1)^2 - \frac{(\Delta\zeta)^2}{[(\Delta\zeta)^2 + \eta]}\frac{A_hA_l}{A_t^2} + (3 - 2\zeta_L)\frac{A_h}{A_t} + 8\pi\frac{\bar\kappa\rho^2}{\kappa A_t} \quad (8)$$

Spherical Micelles. The energy per unit area of spherical micelles of radius ρ derived from (6) as a function of their composition ϕ_s is

$$f_s = [(\Delta\zeta)^2 + \eta]\phi_s^2 + (2\zeta_L\Delta\zeta - \eta - 4\Delta\zeta)\phi_s + 4 - 4\zeta_L + 2\frac{\bar\kappa}{\kappa} + \zeta_L^2 \quad (9)$$

Flat Bilayer of a Liposome. The energy per unit area of a monolayer of a flat bilayer f_b as a function of its composition ϕ_b is given by

$$f_b = [(\Delta\zeta)^2 + \eta]\phi_b^2 + (2\zeta_L\Delta\zeta - \eta)\phi_b + \zeta_L^2 \quad (10)$$

Liposomes to Micelles Transition. We analyze the transition from liposomes to micelles by the Gibbs graphical method, illustrated in Figure 3 for one particular set of parameters of the system. The energies of the pure phases (7)−(10) are convex functions of composition as presented by the curves b, c, and d for the bilayers (liposomes), cylindrical micelles, and disklike micelles, respectively. The energies of mixtures of coexisting phases are presented by common tangents (dashed lines in Figure 3). Compositions ϕ^* at the points where the common tangents touch the energy of bilayers (curve b) indicate phase transitions. We denote the compositions determining the transitions of liposomes to cylindrical, disklike, and spherical micelles by ϕ^*(b→c), ϕ^*(b→d), and ϕ^*(b→s), respectively.

The micelles for which the composition of transition ϕ^* has the lowest value are expected to be formed upon solubilization.

The details on determination of the compositions of transition on the basis of eqs 7−10 are described in Appendix D.

We obtain for the transitions from bilayers to cylindrical micelles

$$\frac{\eta + (\Delta\zeta)^2}{\eta}[\zeta_L + \Delta\zeta\phi^*(\text{b}\rightarrow\text{c})] = \frac{1}{2} + \frac{A_h}{A_h + A_t} + \frac{\bar\kappa}{\kappa}\frac{\eta + (\Delta\zeta)^2}{\eta}\frac{4\pi\rho^2}{A_h + A_t} \quad (11)$$

for the transitions from bilayers to disklike micelles,

$$\frac{\eta + (\Delta\zeta)^2}{\eta}[\zeta_L + \Delta\zeta\phi^*(\text{b}\rightarrow\text{d})] = \frac{1\langle J^2\rangle}{2\langle J\rangle} + \frac{\bar\kappa}{\kappa}\frac{\eta + (\Delta\zeta)^2}{\eta}\frac{4\pi\rho^2}{A_e\langle J\rangle} \quad (12)$$

and for the transition from bilayers to spherical micelles,

$$\frac{\eta + (\Delta\zeta)^2}{\eta}[\zeta_L + \Delta\zeta\phi^*(\text{b}\rightarrow\text{s})] = 1 + \frac{1\bar\kappa}{2\kappa}\frac{\eta + (\Delta\zeta)^2}{\eta} \quad (13)$$

Criteria for the Shape of Micelles

To compare the critical compositions given by eqs 11−13, we use the expressions for A_e, $\langle J^2\rangle$, and $\langle J\rangle$ derived in Appendix A.

It follows from (11)−(13) that the type of the formed micellar phase is controlled by a unique parameter,

$$\lambda = \frac{\bar\kappa}{\kappa}\frac{\eta + (\Delta\zeta)^2}{\eta} \quad (14)$$

To illustrate it, we show in Figure 4 (A−C) the dependence of the critical composition for the transitions of the bilayer into cylindrical micelles ϕ^*(b→c) and into disklike micelles ϕ^*(b→d) as functions of the micellar area A_t for different values of λ ($\lambda = -0.3$ in panel A, $\lambda = -0.6$ in panel B, $\lambda = -2.$ in panel C).

For comparison, we show in the same figure the critical composition for the transition into spherical micelles ϕ^*(b→s) presented as a constant dashed line as the size of micelles of this type is fixed. As obvious from Figure 4, for $\lambda = -0.3$

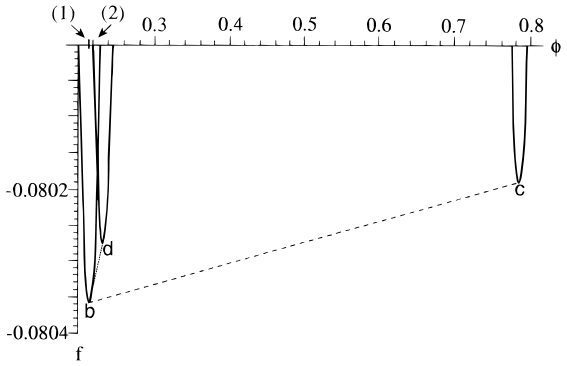

Figure 3. Free energies of the different states of the system: liposomes (bilayers) (curve b, according to eq 10), disklike micelles (curve d, according to eq 7), cylindrical micelles (curve c, according to eq 8), the phase of coexisting liposomes and disklike micelles (common tangent b−d), the phase of coexisting liposomes and cylindrical micelles (common tangent b−c). The chosen parameters on the curves are $\eta = 0.75$, $\Delta\zeta = 1.0$, $\zeta_L = 0$, $\bar{\kappa} = 0$, the radius of a disklike micelle $R = 100\rho$, the length of a cylindrical micelle $l = 10000\rho$. Points 1 and 2 on the ϕ-axis indicate the critical compositions ϕ^*(b→d) and ϕ^*(b→c), respectively.

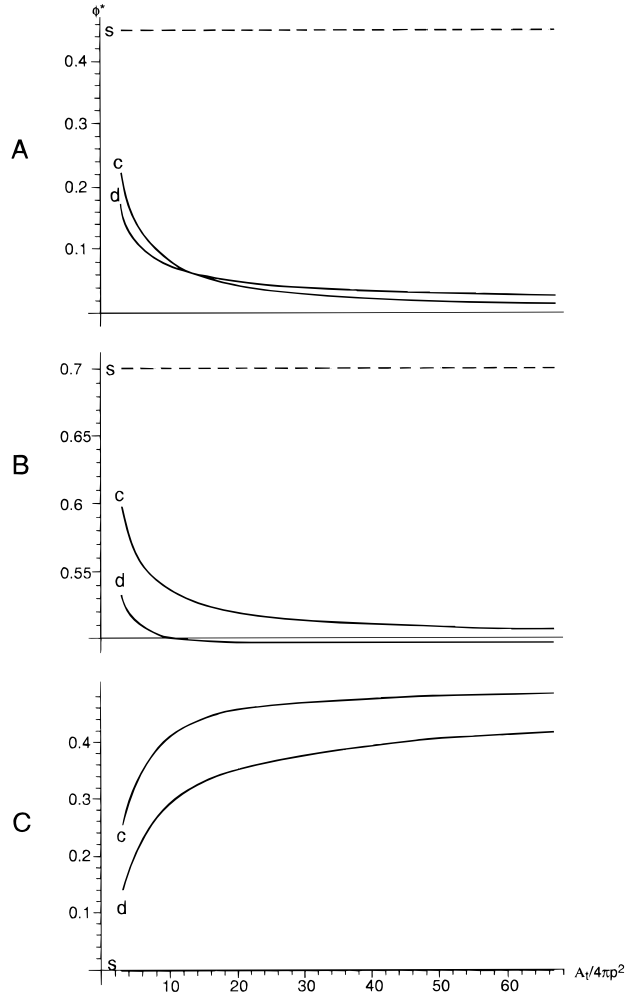

Figure 4. Critical compositions of transition of liposomes into disklike micelles (ϕ^*(b→d), curve d according to eq 12) and into cylindrical micelles (ϕ^*(b→c), curve c according to eq 11) as functions of surface area of one micelle for different values of the parameter λ. (For comparison, the dashed line s (eq 13) shows the constant critical composition of transition of liposomes to spherical micelles (ϕ^*(b→s).) (A) $\lambda = -0.3$; (B) $\lambda = -0.6$; (C) $\lambda = -2$.

(Figure 4A) the lowest critical composition corresponds to the transition into long cylindrical micelles; for $\lambda = -0.6$ (Figure 4B) the lowest critical composition corresponds to the transitions into the disklike micelles of finite area; and, finally, in the case $\lambda = -2$. (Figure 4C) the lowest critical composition is equal to zero and corresponds to the transition into spherical micelles.

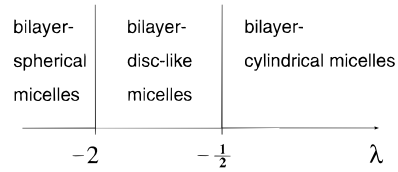

Figure 5. Phase diagram of the shapes of micelles resulting from solubilization of bilayers (liposomes) at different values of parameter λ.

Detailed analysis of the model shows that there are two values of the parameter λ, equal to $\lambda_1 = -1/2$ and $\lambda_2 = -2$, that separate the solubilization of the bilayer into three different regimes. For

$$\lambda > -1/2 \tag{15}$$

the phase transition results in formation of long cylindrical micelles; for

$$-2 < \lambda < -1/2 \tag{16}$$

the transition leads to formation of disklike micelles of a finite radius, while for

$$\lambda < -2 \tag{17}$$

the bilayer transforms into spherical micelles. This is illustrated in Figure 5, which shows the type of phase transition for different values of the parameter λ.

Discussion

We have shown that the type of micelles resulting from solubilization of bilayers is determined by the value of the parameter λ (14). This parameter depends on the difference of spontaneous curvatures of surfactant and lipid $\Delta c = c_D - c_L$, the bending rigidity κ, the Gaussian curvature modulus $\bar{\kappa}$, and the temperature T:

$$\lambda = \frac{\bar{\kappa}}{\kappa}\frac{k_B T + (1/4)\kappa a_L(\Delta c)^2}{k_B T} \tag{18}$$

To understand qualitatively these results, let us recall that according to the model of membrane elasticity,[22] the Gaussian curvature modulus $\bar{\kappa}$, which controls the tendency of the monolayer to change its topology, can be either positive or negative. Negative values of $\bar{\kappa}$ favor the division of each closed monolayer into a large as possible number of separated closed monolayers, whereas positive values of $\bar{\kappa}$ result in the opposite tendency, i.e. in recombination of separated membranes into a single one. Hence, negative values of $\bar{\kappa}$ (yielding negative values of λ) prefer a large number of relatively small disklike or spherical micelles rather than a fewer long cylindrical micelles. An opposite tendency competing with the effects of the negative $\bar{\kappa}$ relates to the energy of bending. This energy is controlled by the bending modulus κ, the difference in spontaneous curvatures of the components Δc, and the effectiveness of repartitioning of the surfactant between the parts of the monolayers with different curvature, which, in turn, is determined by the temperature T. The competition between these tendencies is expressed by the parameter λ (18) and criteria (15)−(17).

Most of the parameters needed to estimate λ are known or can be estimated with reasonable accuracy. We will assume an area per lipid molecule $a_L = 0.6$ nm^2, a radius of curvature of micelles $\rho = 1.5$ nm, a bending modulus of the monolayer $\kappa = 10k_BT$ (at room temperatures), a spontaneous curvature of lipid $c_L = 0$, and a spontaneous curvature of the surfactant $c_D = 1/\rho$.

In the absence of a reliable experimental value for the modulus of Gaussian curvature of the monolayer $\bar{\kappa}$, we refer to the theoretical prediction of $\bar{\kappa}$, as derived from recently developed models[25,29] which predict $\bar{\kappa}$ to be negative and quite small in its absolute value.

With these estimates we can re-express criteria (15)−(17) in terms of the value of the Gaussian curvature modulus $\bar{\kappa}$. In particular, formation of disklike micelles occurs only when

$$\bar{\kappa}/\kappa < -0.2 \tag{19}$$

Numerical calculations[25] performed on lipids and surfactants with usual characteristics give larger values of $\bar{\kappa}$ than required by (19). Therefore, formation of disklike micelles seems to be a very rare event occurring only for lipid/surfactant mixtures with unusual properties. This prediction is in agreement with recent experimental results. However, we note that molecules with highly negative $\bar{\kappa}$, which satisfy (19), can exist. For such compounds, formation of disklike micelles should be expected.[30]

In conclusion, the present model provides the basis for understanding the surfactant-induced transformation of bilayers into various types of mixed micelles. Nonetheless, predictions based on this model should be considered as qualitative rather than quantitative ones. Further development of the model requires more detailed experimental information on the elastic properties of mixed amphiphilic monolayers.

Acknowledgment. We would like to thank R. Granek, W. Helfrich, and S. Safran for stimulating discussions. Support from the German-Israeli Foundation (GIF) under Grant No.I-0197 and the Deutsche Forschungsgemeinschaft through SFB 312 is gratefully acknowledged.

Appendix A: Geometrical Model of Disklike Micelles

We model the rim of a disklike micelle as a surface of revolution of a semicircle about a vertical axis, as illustrated in Figure 1.

The total curvature of the rim $c_m + c_p$ depends on the position along the surface determined by the angle α (Figure 1). Indeed, one principal curvature (meridional curvature) is constant,

$$c_m = 1/\rho \tag{A1}$$

while the second one (parallel curvature) is given by

$$c_p = \frac{1}{\rho}\frac{\cos\alpha}{\cos\alpha + R/\rho} \tag{A2}$$

and changes on the rim.

The resulting dimensionless total curvature is

$$J = \frac{2\cos\alpha + R/\rho}{\cos\alpha + R/\rho} \tag{A3}$$

The element of the area of the rim is

$$dA_e = 2\pi\rho^2\left(\frac{R}{\rho} + \cos\alpha\right)d\alpha \tag{A4}$$

and the total area of a circular rim is

$$A_e = 4\pi\rho^2\left(1 + \frac{\pi}{2}\frac{R}{\rho}\right) \tag{A5}$$

Averaging the curvature and its square over the area of the rim gives

$$\langle J\rangle = \frac{\pi/2 + 2(\rho/R)}{\pi/2 + \rho/R} \tag{A6}$$

$$\langle J^2\rangle = \frac{2(\rho/R)}{\pi/2 + \rho/R}\left[2 + \frac{1}{(\rho/R)\sqrt{1-(\rho/R)^2}}tg^{-1}\sqrt{\frac{1-\rho/R}{1+\rho/R}}\right] \tag{A7}$$

Appendix B: Energy of Phase of Disklike Micelles

We consider the free energy of disklike micelles. The shape of one micelle is illustrated in Figure 1. The area of the monolayer forming the rim of a micelle and that forming the flat central part are denoted by A_e and A_f, respectively. The composition of a micelle averaged over its entire area is ϕ_D.

The free energy of a micelle is equal to the sum of the free energies of the rim and of the flat part. Let us consider them separately.

The free energy per unit area of the rim given by (6) and, accounting for (3) and (4), can be written in dimensionless form as

$$f = (J - \zeta_L - \phi\Delta\zeta)^2 + \eta\phi(\phi - 1) \tag{B1}$$

where J and ϕ are, respectively, the local values of the curvature and composition. We will add later the Gaussian curvature term, as its integral over the micellar closed surface is equal to $8\pi\bar{\kappa}/\kappa$.

The composition of the rim averaged over its area will be denoted as $\langle\phi\rangle = \phi_e$. Minimizing the energy (A1) at fixed average composition ϕ_e, we find the distribution of the composition along the surface of the rim:

$$\phi = \phi_e + \frac{\Delta\zeta}{(\Delta\zeta)^2 + \eta}(J - \langle J\rangle) \tag{B2}$$

Accordingly,

$$\langle\phi^2\rangle = \phi_e^2 + \frac{(\Delta\zeta)^2}{[(\Delta\zeta)^2 + \eta]^2}(\langle J^2\rangle - \langle J\rangle^2) \tag{B3}$$

and

$$\langle J\phi\rangle = \phi_e\langle J\rangle + \frac{(\Delta\zeta)}{(\Delta\zeta)^2 + \eta}(\langle J^2\rangle - \langle J\rangle^2) \tag{B4}$$

Averaging the free energy (B1) over the area of the rim and accounting for the equations (B2)−(B4), we obtain

$$f_e = \zeta_L^2 + \langle J^2\rangle + [(\Delta\zeta)^2 + \eta]\phi_e^2 - 2(\zeta_L + \Delta\zeta\phi_e)\langle J\rangle - \frac{(\Delta\zeta)^2}{(\Delta\zeta)^2 + \eta}(\langle J^2\rangle - \langle J\rangle^2) + (2\zeta_L\Delta\zeta - \eta)\phi_e \tag{B5}$$

The free energy per unit area for the flat central part of a micelle (6) in a dimensionless form is

$$f_f = [(\Delta\zeta)^2 + \eta]\phi_f^2 + (2\zeta_L\Delta\zeta - \eta)\phi_f + \zeta_L^2 \tag{B6}$$

where ϕ_f is the composition of the flat part.

The total energy of a micelle is

$$F_D = f_e A_e + f_f A_f \quad \text{(B7)}$$

while the compositions of the rim and the flat part satisfy the condition

$$\phi_e A_e + \phi_f A_f = \phi_D A_t \quad \text{(B8)}$$

where $A_t = A_e + A_f$ is the total area of the monolayer forming the micelle. Minimizing the free energy (B7) and taking into account (B8), we obtain

$$\phi_e = \phi_D + \frac{\Delta\zeta}{(\Delta\zeta)^2 + \eta}\langle J\rangle\frac{A_f}{A_t} \quad \text{(B9)}$$

and

$$\phi_f = \phi_D - \frac{\Delta\zeta}{(\Delta\zeta)^2 + \eta}\langle J\rangle\frac{A_e}{A_t} \quad \text{(B10)}$$

The resulting expression for the free energy of a micelle is

$$F_d = A_t f_D \quad \text{(B11)}$$

where f_D is the free energy of disklike micelles per unit area given by (7).

The expressions for $\langle J\rangle$, $\langle J^2\rangle$, A_e, and A_t for a specific model of micelle shape used here are derived in Appendix A.

Appendix C: Energy of the Phase of Cylindrical Micelles

The shape of a cylindrical micelle is assumed to consist of cylindrical body of length l and area A_l and two spherical caps of total area A_h. The radius of the cylinder and the caps are assumed to be equal to ρ. Here, their area is equal to $A_l = 2\pi\rho l$ and $A_h = 4\pi\rho^2$, respectively (Figure 2).

The composition of a cylindrical micelle averaged over its area will be denoted as ϕ_c, while ϕ_h and ϕ_l are the compositions of the caps and cylindrical body of a micelle. In analogy with the calculation performed in Appendix B, the dimensionless free energy of a micelle is

$$f_c = A_h[(2 - \zeta_L - \Delta\zeta\phi_h)^2 + \eta\phi_h{}^2 - \eta\phi_h] + A_l[(1 - \zeta_L - \Delta\zeta\phi_l)^2 + \eta\phi_l{}^2 - \eta\phi_l] + 8\pi\frac{\bar{\kappa}}{\kappa}\rho^2 \quad \text{(C1)}$$

The compositions ϕ_e and ϕ_l are related to the average composition ϕ_c by

$$\phi_h A_h + \phi_l A_l = \phi_c A_t \quad \text{(C2)}$$

Minimization of the energy (C1) while accounting for (C2) results in expressions for the compositions of the caps and the cylindrical part:

$$\phi_h = \phi_c + \frac{\Delta\zeta}{(\Delta\zeta)^2 + \eta}\frac{A_l}{A_t} \quad \text{(C3)}$$

$$\phi_l = \phi_c - \frac{\Delta\zeta}{(\Delta\zeta)^2 + \eta}\frac{A_h}{A_t} \quad \text{(C4)}$$

Inserting (C3) and (C4) into (C1), we get the dimensionless free energy of a cylinder micelle,

$$F_c = A_t f_c \quad \text{(C5)}$$

where f_c given by (8) is the free energy per unit area of surface of cylindrical micelles.

In analogy with the derivations above we obtain the expressions (9) and (10) for the free energies of spherical micelles and flat bilayers.

Appendix D: Derivation of Compositions of Phase Transition by Common Tangent Construction

The compositions of bilayers determining their transition to micelles satisfy the conditions of equal $\partial f/\partial\phi$ and equal $f - \phi(\partial f/\partial\phi)$ in both phases. Hence, the expressions necessary to determine these compositions are

$$\frac{\partial f_D}{\partial \phi_D} = 2[(\Delta\zeta)^2 + \eta]\phi_D + \left(2\zeta_L\Delta\zeta - \eta - 2\frac{A_e}{A_t}\Delta\zeta\langle J\rangle\right) \quad \text{(D1)}$$

$$f_D - \phi_D\frac{\partial f_D}{\partial \phi_D} = -[(\Delta\zeta)^2 + \eta]\phi_D{}^2 + \zeta_L{}^2 + \frac{A_e}{A_t}\left[\frac{\eta}{\eta + (\Delta\zeta)^2}\langle J^2\rangle + \frac{(\Delta\zeta)^2}{\eta + (\Delta\zeta)^2}\langle J\rangle^2\right] - \frac{A_e A_f}{A_t{}^2}\frac{(\Delta\zeta)^2}{\eta + (\Delta\zeta)^2}\langle J\rangle^2 - 2\frac{A_e}{A_t}\zeta_L\langle J\rangle + 8\pi\frac{\bar{\kappa}\rho^2}{\kappa A_t} \quad \text{(D2)}$$

$$\frac{\partial f_c}{\partial \phi_c} = 2[(\Delta\zeta)^2 + \eta]\phi_c + 2\zeta_L\Delta\zeta - \eta - 2\Delta\zeta - 2\Delta\zeta\frac{A_h}{A_t} \quad \text{(D3)}$$

$$f_c - \phi_c\frac{\partial f_c}{\partial \phi_c} = -[(\Delta\zeta)^2 + \eta]\phi_c{}^2 + (\zeta_L - 1)^2 - \frac{(\Delta\zeta)^2}{[(\Delta\zeta)^2 + \eta]}\frac{A_h A_l}{A_t{}^2} + (3 - 2\zeta_L)\frac{A_h}{A_t} + 8\pi\frac{\bar{\kappa}\rho^2}{\kappa A_t} \quad \text{(D4)}$$

$$\frac{\partial f_s}{\partial \phi_s} = 2[(\Delta\zeta)^2 + \eta]\phi_s + (2\zeta_L\Delta\zeta - \eta - 4\Delta\zeta) \quad \text{(D5)}$$

$$f_s - \phi_s\frac{\partial f_s}{\partial \phi_s} = -[(\Delta\zeta)^2 + \eta]\phi_s{}^2 + 4 - 4\zeta_L + 2\frac{\bar{\kappa}}{\kappa} + \zeta_L{}^2 \quad \text{(D6)}$$

$$\frac{\partial f_b}{\partial \phi_b} = 2[(\Delta\zeta)^2 + \eta]\phi_b + (2\zeta_L\Delta\zeta - \eta) \quad \text{(D7)}$$

$$f_b - \phi_b\frac{\partial f_b}{\partial \phi_b} = -[(\Delta\zeta)^2 + \eta]\phi_b{}^2 + \zeta_L{}^2 \quad \text{(D8)}$$

References and Notes

(1) Tanford, C. *The Hydrophobic Effect—Formation of Micelles and Biological Membranes*, 2nd ed.; John Wiley and Sons: New York, 1980.

(2) Israelachvili, J. N.; Mitchell, D. J.; Ninham, B. W. *J. Chem. Soc., Faraday Trans. 2* **1976**, *72*, 1521.

(3) Israelachvili, J. N.; Marcelja, S.; Horn, R. G. *Q. Rev. Biophys.* **1980**, *13*, 121.

(4) Gelbart, W. M., Roux, D., Ben-Shaul, A., Eds. *Modern Ideas and Problems in Amphiphilic Sciences*; Springer, Berlin, 1993.

(5) Lichtenberg, D. In *Handbook of Nonmedical Applications of Liposomes*; Barenholz, Y., Lasic, D. D., Eds.; CRC Press: Boca Raton, FL, 1996; Vol. II.

(6) Andelman, D.; Kozlov, M. M.; Helfrich, W. *Europhys. Lett.* **1994**, *25*, 231.

(7) Fattal, D. R.; Andelman, D.; Ben-Shaul, A. *Langmuir* **1995**, *11*, 1154.

(8) Schurtenberger, P.; Mazer, N. A.; Kanzig, W. *J. Phys. Chem.* **1985**, *89*, 1042.

(9) Walter, A.; Vinson, P. K.; Kaplun, A.; Talmon, Y. *Biophys. J.* **1991**, *60*, 1315.

(10) Vinson, P. K.; Talmon, Y.; Walter, A. *Biophys. J.* **1989**, *56*, 669. Edwards, K.; Almgren, M.; Bellare, J.; Brown, W. *Langmuir* **1989**, *5*, 473. Edwards, K.; Almgren, M. *J. Colloid Interface Sci.* **1991**, *147*, 1.
(11) Nichols, J. W.; Ozarowski, J. *Biochemistry* **1990**, *29*, 4600.
(12) Pedersen, J. S.; Egelhaaf, S. U.; Schurtenberger, P. *J. Phys. Chem.* **1995**, *99*, 1299. Hjelm, R. P.; Alkan, M. H.; Thiyagarajan, P. *Mol. Cryst. Liq. Cryst.* **1990**, *180A*, 155.
(13) Egelhaaf, S. U.; Schurtenberger, P. *J. Phys. Chem.* **1994**, *98*, 8560.
(14) Ben-Shaul, A.; Rorman, D. H.; Hartland, G. V.; Gelbart, W. M. *J. Phys. Chem.* **1986**, *90*, 5277.
(15) Szleifer, I.; Ben-Shaul, A.; Gelbart, W. M. *J. Chem. Phys.* **1987**, *86*, 7094.
(16) Zoeller, N. J.; Blankschtein, D. *Ind. Eng. Chem. Res.* **1995**, *34*, 4150.
(17) Kekicheff, P.; Tiddy, G. J. T. *J. Phys. Chem.* **1989**, *93*, 2520.
(18) Hyde, S. T. *Pure Appl. Chem.* **1992**, *64*, 1617.
(19) Hyde, S. T. *Colloq. Phys.* **1990**, *C7*, 209.
(20) Fredrickson, G. H. *Macromolecules* **1991**, *24*, 3456.
(21) Daicic, J.; Fogden, A.; Carlsson, I.; Wennerström, H.; Jönsson, B. *Phys. Rev. E* **1996**, *54*, 3984.
(22) Helfrich, W. *Z. Naturforsch.* **1973**, *28(c)*, 693.
(23) Kozlov, M. M.; Leikin, S.; Rand, R. P. *Biophys. J.* **1994**, *67*, 1603.
(24) Leikin, S.; Kozlov, M. M.; Fuller, N. L.; Rand, R. P. *Biophys. J.* **1996**, *71*, 2623.
(25) Szleifer, I.; Kramer, D.; Ben-Shaul, A.; Gelbart, W. M.; Safran, S. A. *J. Chem. Phys.* **1990**, *92*, 6800.
(26) Dan, N.; Safran, S. A. *Europhys. Lett.* **1993**, *21*, 975. Dan, N.; Safran, S. A. *Macromolecules* **1994**, *27*, 5766.
(27) May, S.; Ben-Shaul, A. *J. Chem. Phys.* **1995**, *103*, 3839.
(28) Kozlov, M. M.; Helfrich, W. *Langmuir* **1992**, *8*, 2792.
(29) Safran, S. A. *Statistical Thermodynamics of Surfaces, Interfaces, and Membranes*; Addison-Wesley Publ. *Co.*: Reading, MA, 1994.
(30) Granek, R.; Gelbart, W. M.; Bohbot, Y.; Ben-Shaul, A. *J. Chem. Phys.* **1994**, *101*, 4331.